Journal of Experimental Botany, Vol. 73, No. 3 pp. 835–847, 2022
https://doi.org/10.1093/jxb/erab430 Advance Access Publication 21 September 2021

RESEARCH PAPER

The chromatin remodelling ATPase BRAHMA interacts with GATA-family transcription factor GNC to regulate flowering time in Arabidopsis

Jie Yang[1,*], Yingchao Xu[1,2,*], Jianhao Wang[3], Sujuan Gao[4,5], Yisui Huang[1], Fu-Yu Hung[6], Tao Li[7], Qing Li[8], Lin Yue[3], Keqiang Wu[6,*,†] and Songguang Yang[1,7,†]

[1] Key Laboratory of South China Agricultural Plant Molecular Analysis and Genetic Improvement, Guangdong Provincial Key Laboratory of Applied Botany, South China Botanical Garden, Chinese Academy of Sciences, Guangzhou 510650, China
[2] University of Chinese Academy of Sciences, Chinese Academy of Sciences, Beijing 100049, China
[3] Innovative Center of Molecular Genetics and Evolution, School of Life Sciences, Guangzhou University, Guangzhou, China
[4] College of Light Industry and Food Science, Zhongkai University of Agriculture and Engineering, Guangzhou 510225, China
[5] Academy of Contemporary Agricultural Engineering Innovations, Zhongkai University of Agriculture and Engineering, Guangzhou 510225, China
[6] Institute of Plant Biology, National Taiwan University, Taipei 106, Taiwan
[7] Vegetable Research Institute, Guangdong Academy of Agricultural Sciences, Guangzhou, China
[8] Guangdong Provincial Key Laboratory for Crop Germplasm Resources Preservation and Utilization, Agrobiological Gene Research Center, Guangdong Academy of Agricultural Sciences, Guangzhou, China

* These authors contributed equally to this work.
† Correspondence: yangsongguang@scbg.ac.cn or kewu@ntu.edu.tw

Received 3 July 2021; Editorial decision 14 September 2021; Accepted 20 September 2021

Editor: Rainer Melzer, University College Dublin, Ireland

Abstract

BRAHMA (BRM) is the ATPase of the SWItch/Sucrose Non-Fermentable (SWI/SNF) chromatin remodelling complex, which is indispensable for transcriptional inhibition and activation, associated with vegetative and reproductive development in *Arabidopsis thaliana.* Here, we show that BRM directly binds to the chromatin of *SUPPRESSOR OF OVEREXPRESSION OF CONSTANS 1* (*SOC1*), which integrates multiple flowering signals to regulate floral transition, leading to flowering. In addition, genetic and molecular analysis showed that BRM interacts with GNC (GATA, NITRATE-INDUCIBLE, CARBON METABOLISM INVOLVED), a GATA transcription factor that represses flowering by directly repressing *SOC1* expression. Furthermore, BRM is recruited by GNC to directly bind to the chromatin of *SOC1*. The transcript level of *SOC1* is elevated in *brm-3*, *gnc,* and *brm-3*/*gnc* mutants, which is associated with increased histone H3 lysine 4 tri-methylation (H3K4Me3) but decreased DNA methylation. Taken together, our results indicate that BRM associates with GNC to regulate *SOC1* expression and flowering time.

Keywords: BRAHMA (BRM), chromatin remodelling, flowering time, GNC (GATA, NITRATE-INDUCIBLE, CARBON METABOLISM INVOLVED), SUPPRESSOR OF OVEREXPRESSION OF CONSTANS 1 (SOC1).

Introduction

ATP-dependent chromatin remodelling complexes (CRCs) regulate gene expression by modulating chromatin architecture (Clapier and Cairns, 2009; Ho and Crabtree, 2010; Hargreaves and Crabtree, 2011; Clapier *et al.*, 2017). CRCs destabilize DNA–histone interactions by using the energy from ATP hydrolysis to translocate, evict, or change the composition of nucleosomes (Clapier *et al.*, 2017). CRCs can be classified into four groups based on their ATPase subunits: SWItch/Sucrose Non-Fermentable (SWI/SNF), Imitation Switch (ISWI), Mi-2/chromodomain helicase DNA-binding 1 (Mi-2/CHD1), and Inositol Requiring 80 (INO80) (Vignali *et al.*, 2000). SWI/SNF-type CRCs contain several subunits, including four SWI2/SNF2 ATPases (BRAHMA, SPLAYED, CHROMATIN REMODELING 12 and 23), four SWI3 proteins (SWI3A to SWI3D), two SWI/SNF ASSOCIATED PROTEINS 73 (SWP73A and SWP73B), two ACTIN RELATED PROTEINS (ARP4 and ARP7), and a single SNF5 subunit (BUSHY; BSH) (Vercruyssen *et al.*, 2014; Sarnowska *et al.*, 2016).

The SWI2/SNF2 ATPase BRM plays an essential role in *Arabidopsis thaliana* development during embryonic, vegetative, and reproductive growth (Farrona et al., 2004, 2011; Hurtado *et al.*, 2006; Kwon *et al.*, 2006; Jerzmanowski, 2007; Tang *et al.*, 2008; Han *et al.*, 2012; Wu *et al.*, 2012; Zhu *et al.*, 2013; Vercruyssen *et al.*, 2014; Li *et al.*, 2015; Yang *et al.*, 2015; D. Zhang *et al.*, 2017; J. Zhang *et al.*, 2017; Richter *et al.*, 2019). For instance, a loss-of-function mutation in *BRM* results in pleiotropic phenotypes, such as reduced plant size with short roots (Farrona *et al.*, 2004; Hurtado *et al.*, 2006; Yang *et al.*, 2015), downward-curling leaves (Hurtado *et al.*, 2006), hypersensitivity to abscisic acid (Han *et al.*, 2012), and early flowering (Farrona et al., 2004, 2007, 2011; Li *et al.*, 2015). Indeed, both *BRM*-silenced and *brm*-null mutant plants flower earlier and with fewer leaves, compared with the wild type (Farrona *et al.*, 2004; Hurtado *et al.*, 2006). Consistent with this observation, the mRNA levels of *CONSTANS* (*CO*), *FLOWERING LOCUS T* (*FT*), and *SOC1* are significantly higher in *brm* mutant plants than in the corresponding wild types (Farrona *et al.*, 2004). Interestingly, the expression of *FLOWERING LOCUS C* (*FLC*), the key repressor of *FT*, is also significantly higher in *brm* plants (Farrona *et al.*, 2011). Nevertheless, genetic data showed that BRM can control *FT* independent of CO and FLC, and can also control *SOC1* independent of FT (Farrona *et al.*, 2011). Furthermore, BRM acts as a direct upstream activator of *SHORT VEGETATIVE PHASE* (*SVP*), a key flowering repressor gene in Arabidopsis (Li *et al.*, 2015). BRM can reduce the level of histone H3 lysine 27 trimethylation (H3K27Me3) at the *SVP* locus by inhibiting the binding and activities of polycomb group (PcG) proteins (Li *et al.*, 2015). Intriguingly, a recent study demonstrated that BRM and the histone demethylase RELATIVE OF EARLY FLOWERING 6 (REF6) must associate with SOC1 to activate the transcription of *TARGET OF FLC AND SVP1* (*TFS1*), a novel target of FLC and SVP (Richter *et al.*, 2019). SOC1 resolves condensed chromatin structures and opens chromatin at the *TFS1* locus through its combinatorial activity with REF6 and BRM. BRM also regulates flowering, since BRM acts at the nucleosome level to fine-tune the temporal expression of *miR156* (Xu *et al.*, 2016). Taken together, these data demonstrate that BRM is an essential regulator of flowering.

In addition to its role in flowering, BRM is involved in controlling floral organ identity via its interactions with LEAFY (LFY) and SEPALLATA3 (SEP3), while controlling leaf development though interacting with transcription factors TEOSINTE BRANCHED1/CYCLOIDEA/PCF (TCP) family member TCP4 and ANGUSTIFOLIA3 (AN3) (Wu *et al.*, 2012; Efroni *et al.*, 2013; Vercruyssen *et al.*, 2014). BRM also interacts with BREVIPEDICELLUS (BP) to regulate inflorescence architecture (Zhao *et al.*, 2015). Furthermore, BRM binds specifically to the chromatin of several *PINFORMED* loci and activates their expression to maintain the root stem cell niche (Yang *et al.*, 2015). BRM also interacts with PHYTOCHROME INTERACTING FACTOR 1 (PIF1) to regulate *PROTOCHLOROPHYLLIDE OXIDOREDUCTASE C* (*PORC*) expression, with downstream effects on chlorophyll biosynthesis during the transition from heterotrophic to autotrophic growth in seedlings (D. Zhang *et al.*, 2017). Taken together, these findings demonstrate that the SWI/SNF ATPase BRM associates with different transcription factors to modulate gene expression as required for plant development processes.

GATA family transcription factors were first identified to interact with conserved WGATAR (W=T or A; R=G or A) motifs that are involved in erythroid-specific gene expression in vertebrates (Evans *et al.*, 1988; Lowry and Atchley, 2000). The DNA-binding domain of GATA transcription factors is a type IV zinc finger with the form $CX_2CX_{17-20}CX_2C$, followed by a highly basic region (Ko and Engel, 1993). The Arabidopsis genome harbours 29 members of the GATA family, each of which has a highly conserved GATA-type zinc-finger motif (Reyes *et al.*, 2004; Naito *et al.*, 2007). Previous studies showed that two paralogous GATA transcription factors—GATA, NITRATE-INDUCIBLE, CARBON METABOLISM INVOLVED (GNC) and GNC-LIKE/CYTOKININ-RESPONSIVE GATA FACTOR 1 (GNL/CGA1)—are involved in chlorophyll synthesis, chloroplast and stomatal development, glucose sensitivity, senescence, and cytokinin (CK), gibberellin (GA), and light signalling in Arabidopsis (Bi *et al.*, 2005; Naito *et al.*, 2007; Richter et al., 2010; 2013b; Hudson *et al.*, 2011; Chiang *et al.*, 2012; Klermund *et al.*, 2016; Ranftl *et al.*, 2016; Zubo *et al.*, 2018). GNC and GNL control greening by directly increasing the expression of several key enzymes in the chlorophyll- and haem-synthesizing branch of the tetrapyrrole biosynthesis pathway (Bastakis *et al.*, 2018). Furthermore, GNC and GNL act upstream of *SOC1* to directly repress its expression and

thereby repress flowering (Richter *et al.*, 2013*a*). Genetic interaction studies revealed that GNC and GNL act downstream of *SOC1* to control greening and cold tolerance (Richter *et al.*, 2013*a*).

Plants must adapt to their environmental conditions to guarantee optimal reproductive success. Many endogenous signals (e.g. autonomous signals, gibberellin levels, circadian clock inputs, age, and sugar content) and environmental signals (vernalization, ambient temperature, and photoperiod) converge to a few floral integrator genes, such as *FT*, *TWIN SISTER OF FT* (*TSF*), *SOC1*, and *AGAMOUS-LIKE24* (*AGL24;* Spanudakis and Jackson, 2014; Blumel *et al.*, 2015), which signal the transition from vegetative to floral meristems by activating the meristem identity genes *LFY*, *APETALA1* (*AP1*), *SEP3* and *FRUITFULL* (*FUL*). Unlike other floral integrators, SOC1 regulates not only flowering time but also floral patterning, floral meristem determinacy, sugar transport, and stomatal opening (Hepworth *et al.*, 2002; Liu *et al.*, 2009; Richter *et al.*, 2013*b*; Hou *et al.*, 2014; Andrés *et al.*, 2020).

In this work, we report a direct interaction between the Arabidopsis chromatin remodelling ATPase BRM and the GATA family transcription factor GNC, both *in vitro* and *in vivo*. BRM and GNC bind to the promoter and coding region of *SOC1*, serving as negative regulators of flowering time by directly repressing *SOC1* expression. Furthermore, BRM and GNC act together to decrease H3K4Me3 and increase DNA methylation of *SOC1*. Our observations suggest that BRM and GNC may act as a co-repressor complex involved in flowering via repressing *SOC1* in Arabidopsis.

Materials and methods

Plant materials and growth conditions

Arabidopsis plants were grown in peat soil (Hawita-Baltic Traysubstrate, Hawita-Grupe GmbH, Germany) in a growth chamber under long-day conditions (LD, 22 °C, 16 h light/8 h dark, light intensity of 100 μmol m^{-2} s^{-1}). All mutants used in this study are in the Col-0 background. The *BRM* mutant line *brm-3* (SALK_088462) and *GNC* mutant line *gnc* (SALK_001778) were obtained from the Arabidopsis Biological Resource Center (http://www.arabidopsis.org/). The *brm-3/gnc* double mutant was generated by crossing the *brm-3* and *gnc* single mutants. The nutrient source used for sample collection was Murashige and Skoog basal salt mixture (MS) supplemented with 1% sucrose. The *BRMpro:BRM-GFP* transgenic plants have been described previously (Smaczniak *et al.*, 2012) and were obtained from Cui's laboratory. The full-length coding sequences of *BRM* and *GNC* were PCR-amplified from the cDNA of whole seedlings, cloned into the pCAMBIA1302 binary vector, and transformed into the *Agrobacterium tumefaciens* strain EHA105. The *35S:GNC-GFP* (*GNC*-OE) and *35S:BRM-GFP* (*BRM*-OE) transgenic plants were then generated using the floral dip method (Clough and Bent, 1998). All primers used for plasmid construction are listed in Supplementary Table S1.

Phenotypic analysis

Wild-type (Col-0) and mutant plants were grown side by side as described above. The number of rosette leaves was counted when the length of the inflorescence stem began to appear. For chlorophyll quantification, 12-day-old seedlings (about 0.2 g fresh weight) grown on MS plates were collected. Chlorophyll was extracted using 80% acetone and analysed by spectrofluorometry (Porra *et al.*, 1989). For each genotype, at least 20 plants were analysed, and the analysis was repeated three times independently.

Yeast two-hybrid (Y2H) assays

Y2H assays were performed as described in the manual of the GAL4-based Matchmaker Two-Hybrid System 3 (Clontech Laboratories, USA). Full length BRM (1–2193 aa) and different parts of BRM (1–952 aa and 953–2193 aa) coding regions were each fused with pGBKT7-BD to create bait constructs. The prey construct was created by fusing the full-length coding region of *GNC* with the pGADT7-AD vector. The bait and prey constructs were co-transformed into the yeast strain AH109 using the lithium acetate method (Gietz and Woods, 2002), and yeast cells were grown on DDO medium (minimal media double dropouts; SD medium lacking tryptophan and leucine) for 3 d at 28 °C. Transformed colonies were plated onto TDO medium (minimal media triple dropouts; SD medium lacking tryptophan, leucine, and histidine) containing 40 μg ml^{-1} of 5-bromo-4-chloro-3-indoyl-α-D-galactosidase (TDO/X) to test for possible interactions between BRM and GNC.

Luciferase complementation imaging assays

Luciferase complementation imaging (LCI) assays were performed as described previously (Chen *et al.*, 2008). Briefly, the coding region for *BRM-N* (amino acids 1–952) or *GNC* was cloned into pCAMBIA-CLuc and pCAMBIA-NLuc, respectively. Each construct was transformed into *Agrobacterium tumefaciens* strain EHA105. An equal volume of *A. tumefaciens* harbouring pCAMBIA-NLuc and pCAMBIA-CLuc constructs (or the parental plasmids as controls) was mixed, with a final concentration of OD_{600}=1.0. The *A. tumefaciens* mixtures were infiltrated into three leaves of *Nicotiana benthamiana* plants. After the plants had recovered for 60 h at 22 °C, luciferin (100 μM) was sprayed. A low-light, cooled CCD imaging apparatus (Tanon 5200, USA) was used to capture the luciferase image.

In vitro *pull-down assays*

The GST pull-down assay was performed as described previously, with some modifications (Zhao *et al.*, 2015). The coding region of *GNC* was cloned into pGEX4T-3, and the coding region of *BRM-N* (encoding amino acids 1–952) was cloned into pET28(a). The proteins were expressed at 25 °C for 12 h in *Escherichia coli* BL21 cells supplied with 0.5 mM isopropylthio-β-galactoside. GST or GST-GNC recombinant proteins were incubated with GST resin (GE Healthcare, USA) in a binding buffer (50 mM Tris, pH 7.4; 120 mM NaCl; 5% glycerol; 0.5% Nonidet P-40; 1 mM phenylmethylsulfonyl fluoride; and 1 mM β-mercaptoethanol) for 2 h at 4 °C, and were then collected and mixed with supernatant containing His-BRM_{1-952} protein, and incubated at 30 °C for 60 min. After being rinsed five times with wash buffer (50 mM Tris, pH 7.4, 120 mM NaCl, 5% glycerol, and 0.5% Nonidet P-40), the bound proteins were boiled in sodium dodecyl sulphate (SDS) sample buffer and subjected to SDS-polyacrylamide gel electrophoresis and immunoblotting.

Co-immunoprecipitation (Co-IP) assays

Co-IP assays were performed as described previously (Zhao *et al.*, 2015). *A. tumefaciens* cells harbouring *pEAQ-GFP*, *pEAQ-*BRM_{1-952}*-GFP*, or *pHB-GNC-FLAG* were each infiltrated into at least six tobacco leaves. After 36 h of infiltration, tobacco leaves were harvested and ground to

a fine powder in liquid nitrogen. Proteins were extracted in an extraction buffer (50 mM Tris-HCl, pH 7.4; 150 mM NaCl; 2 mM $MgCl_2$; 1 mM DTT; 20% glycerol; and 1% NP-40) containing a protease inhibitor cocktail (Roche). Cell debris was pelleted by centrifugation at 14 000 × *g*, 4 °C for 20 min. The supernatant was incubated with 30 µl of GFP-Trap®-A beads (Chromo Tek, Germany) at 4 °C for 4 h, following which the beads were centrifuged and washed six times with a washing buffer (50 mM Tris-HCl, pH 7.4; 150 mM NaCl; 2 mM $MgCl_2$; 1 mM DTT; 10% glycerol; and 1% NP-40). Proteins were eluted with 40 µl of 2× loading buffer and analysed by immunoblotting using anti-GFP (HT801-01, TransGen, China) and anti-FLAG antibodies (HT201-01, TransGen, China).

RT–qPCR analysis

Total RNA from 12-day-old seedlings grown on MS medium was extracted using HiPure Plant RNA Mini Kit (Magen, China) and subjected to cDNA synthesis. About 2 µg total RNA was used to generate cDNA using the TransScript® One-Step gDNA Removal and cDNA Synthesis SuperMix (TransGen, China) according to the manufacturer's instructions. As a template, 150 ng of synthesized cDNA was used to perform RT–qPCR analysis. PCR reactions were performed in a total volume of 10 µl, with 0.5 µl of each primer (final concentration 100 nM) and 5 µl of SYBR Green PCR Super mix (Bio-Rad Laboratories, USA) on an ABI7500 Real-Time PCR System (Applied Biosystems, USA). The PCR program included an initial denaturation step at 94 °C for 3 min, followed by 40 cycles of 30 s at 94 °C and 35 s at 60 °C. Each sample was quantified in triplicate and normalized using *UBIQUITIN 10* (*UBQ10*) or *ACTIN2* as internal controls. Three biological replicates were performed, and three to four technical repeats were performed for each biological replicate. The primer pairs for RT–qPCR are listed in Supplementary Table S1.

Transient transactivation assays

To study the transcriptional activation of *SOC1* by BRM and GNC, the *SOC1* promoter was cloned into a pGreenII 0800-LUC double-reporter vector ($SOC1_{pro}$-LUC; Hellens *et al.*, 2005), while $BRM_{1\text{-}952}$ and *GNC* were cloned into pEAQ-GFP (Sainsbury *et al.*, 2009) and pHB-FLAG (Mao *et al.*, 2005) effector vectors, respectively. The constructed effector (pEAQ-$BRM_{1\text{-}952}$-GFP and pHB-*GNC*-FLAG) and reporter ($SOC1_{pro}$-LUC) plasmids were co-transformed into tobacco by *A. tumefaciens* strain EHA105, as described above. LUC and REN luciferase activities were measured using the dual luciferase assay kit (E1910, Promega, United States). The analysis was executed using the Luminoskan Ascent Microplate Luminometer (Thermo Fisher Scientific, USA) according to the manufacturer's instructions. The results were determined by calculating the ratio of LUC to REN. The primers used for transient activation assay are shown in Supplementary Table S1.

Chromatin immunoprecipitation (ChIP) assays

The ChIP assays were performed as described previously (Gendrel *et al.*, 2005). Chromatin extracts were prepared from 12-day-old seedlings treated with 1% formaldehyde. The chromatin was sheared to an average length of 800 bp by sonication, and immunoprecipitated with specific antibodies: anti-H3K4Me3 (Millipore, 07-473, USA), anti-H3K27Me3 (Millipore, 07-449, USA), and anti-GFP (Sigma, 6795, USA). The DNA cross-linking to the immunoprecipitated proteins was reversed, and then the immunoprecipitation of targets of interest was quantified with RT-qPCR. The gene-specific primers used are listed in Supplementary Table S1. Three biological replicates were performed, and three to four technical repeats were carried out for each biological replicate.

Methyl-DNA immunoprecipitation–qPCR (MeDIP-qPCR) assays

The MeDIP-qPCR assays were performed as described previously (Yang *et al.*, 2020). Genomic DNA was extracted from 12-day-old Col-0, *brm-3*, *gnc*, and *brm-3/gnc* seedlings and was sonicated to create random fragments ranging in size from 300–1000 bp. Subsequently, DNA was denatured in boiling water and incubated overnight at 4 °C with a monoclonal antibody against 5-methylcytidine (5-mC) (Abcam, ab10805, UK). Enriched MeDIP fragments were measured by qPCR, and a portion of the untreated, sonicated DNA was used as an input control. The primers used for methylated DNA immunoprecipitation-qPCR analysis are listed in Supplementary Table S1. Three biological replicates were performed, and three to four technical repeats were carried out for each biological replicate.

Statistical analysis

Data represent means ±SE. A Student's *t*-test was used for comparisons between two samples, and differences between treatments were analysed with a one-way ANOVA at the $P \leq 0.05$ level of significance. Statistical analyses were performed using the SPSS statistical software (SPSS 16.0, SPSS Inc., Chicago, IL, USA).

Results

BRM interacts with GNC in vitro *and* in vivo

Previous studies demonstrated that both BRM and GNC can repress *SOC1* expression (Farrona *et al.*, 2004; Richter *et al.*, 2013*b*). To analyse whether BRM can directly interact with GNC, we performed yeast two-hybrid (Y2H) assays. Yeast cells co-transformed with *AD-GNC* (the full-length coding region sequence of *GNC* fused to pGAKT7) and *BD-BRM* (the full-length coding region sequence of *BRM* fused to pGBKT7) could grow on the selective medium (TDO/X), indicating that BRM directly interacted with GNC in yeast cells (Fig. 1A). Further Y2H experiments showed that the N terminus of BRM (amino acids 1–952) was responsible for their interaction (Fig. 1A), which was consistent with previous reports (Farrona *et al.*, 2004; Zhao *et al.*, 2015). Intriguingly, GNL/CGA1, the homolog of GNC, did not interact with BRM in yeast cells (Supplementary Fig. S1). We confirmed the interaction between BRM and GNC using *in vitro* GST pull-down assays. Purified BRM-His (1–952 aa) was pulled down by GST-GNC, but not GST alone, confirming that BRM physically interacts with GNC *in vitro* (Fig. 1B).

We further examined the interaction between BRM and GNC *in vivo* using luciferase complementation imaging (LCI) and co-immunoprecipitation (co-IP) assays. For the LCI assays, *GNC* and the N-terminus of *BRM* (encoding amino acids 1–952) were fused to the NLuc vector and CLuc vector, respectively (Chen *et al.*, 2008). The constructs were infiltrated into *Nicotiana benthamiana* leaves. There was strong LUC activity when $BRM_{1\text{-}952}$-Cluc and GNC-Nluc were co-expressed (Fig. 1C), indicating that the N-terminus of BRM interacted with GNC in plant cells, consistent with the *in vitro* results. For the co-IP assays, $BRM_{1\text{-}952}$-GFP and

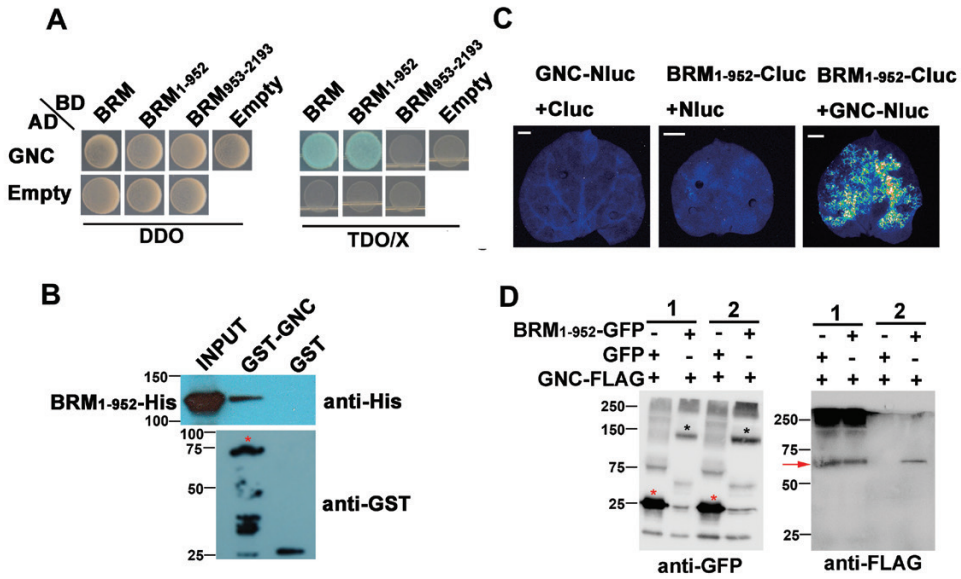

Fig. 1. BRM interacts with GNC *in vitro* and *in vivo*. (A) Yeast-two-hybrid analysis of the interaction between BRM and GNC. The different sequences of *BRM* and the full-length coding sequence of *GNC*, fused with GAL4 activation domain (*AD*) and GAL4 DNA binding domain (*BD*) vectors, respectively, were co-transformed into yeast cells and plated on DDO medium. The transformants were then plated on TDO/X medium at 30 °C to test for possible interaction. DDO, minimal media double dropouts and the SD medium lacking tryptophan and leucine. TDO, minimal media triple dropouts and SD medium lacking tryptophan, leucine and histidine. TDO/X, TDO medium containing 40 μg ml^{-1} of 5-bromo-4-chloro-3-indoyl-α-D-galactosidase. (B) The interaction between BRM and GNC was confirmed by *in vitro* pull-down assays. The N-terminus of BRM (amino acids 1–952) fused with a His tag was incubated with immobilized GST-GNC or GST (control). The precipitated N-BRM was detected by anti-His antibody in immunoblotting. The protein levels of GST-GNC and GST are shown at the bottom. The molecular weight (kDa) is indicated in the right panel. The red asterisk indicates GST-GNC. (C) LCI analysis of the interaction of BRM and GNC. The *Agrobacterium* carrying the indicated construct pairs were injected into tobacco leaves, and the LUC image was captured 60 h after injection. Scale bar =1 cm. (D) The interaction between the GNC and N-terminus of BRM (1–952aa) in an *in vivo* co-IP assay. The *GFP*, $BRM_{1\text{-}952}$*-GFP* and *GNC-FLAG* co-expressed in tobacco leaves by *Agrobacterium* injection. Total protein extracts were immunoprecipitated with the immobilized anti-GFP antibody (marked as 2), and the immunoprecipitated protein was then detected by western blotting assays using an anti-FLAG antibody. Input BRM (1–952aa)-GFP and GNC-FLAG proteins (marked as 1) were detected with anti-GFP and anti-FLAG antibodies, respectively. The molecular weight (kDa) is indicated in right panel. The red and black asterisks indicate GFP and $BRM_{1\text{-}952}$-GFP, respectively, while the red arrow indicates GNC-FLAG.

GNC-FLAG constructs were co-expressed in *N. benthamiana* leaves. We immunoprecipitated proteins from the leaves using an anti-GFP antibody and analysed samples by immunoblotting with an anti-FLAG antibody. As shown in Fig. 1D, the GNC-FLAG was co-immunoprecipitated by $BRM_{1\text{-}952}$-GFP. Collectively, these experiments demonstrate that BRM interacts with GNC both *in vivo* and *in vitro*.

BRM and GNC act together to regulate flowering time

Previous studies demonstrated that *brm-1* and *brm-2* plants flower early under long-day (LD: 16 h light/8 h dark) conditions (Farrona *et al.*, 2004; 2011). Two other T-DNA insertion mutants, *brm-3* (Tang *et al.*, 2008) and *brm-20* (D. Zhang *et al.*, 2017), also displayed an early flowering phenotype under LD conditions (Supplementary Fig. S2). We were interested in establishing whether the interaction between BRM and GNC influences this early flowering phenotype. So we generated a *brm-3/gnc* double mutant by crossing *brm-3* and *gnc* plants. As shown in Fig. 2A, the *brm-3/gnc* double mutant displayed an earlier flowering phenotype under LD conditions compared with either the single mutants or the corresponding wild type (Col-0). We also compared the number of leaves in the rosette at flowering time for the *brm-3*, *gnc,* and *brm-3/gnc* mutants under LD. As previously reported (Li *et al.*, 2015; Richter *et al.*, 2013*a*), the *brm-3* and *gnc* mutants had fewer rosette leaves than Col-0 plants under LD conditions, and the *brm-3/gnc* double mutant had fewer rosette leaves than either single mutant (Fig. 2B). These data indicated that BRM and GNC act additively to regulate flowering time under LD. Intriguingly, like *brm-3*, *brm-3/gnc* showed twisted cauline leaves under LD conditions (Fig. 2A), indicating that BRM acts downstream of GNC in leaf development.

Next, we crossed *brm-3* plants with plants that overexpress GFP-tagged GNC (*GNC*-OE) to create double mutants. RT–qPCR data confirmed that *GNC* was overexpressed in *GNC*-OE and *GNC*-OE/*brm-3* plants, compared with Col-0 (Supplementary Fig. S3). *GNC*-OE plants showed a strong delayed flowering phenotype (Fig. 2C, D), consistent with previous reports (Richter *et al.*, 2013*a*). In contrast, flowering time of *GNC*-OE/*brm-3* plants was considerably earlier than that of Col-0 and *GNC-OE* under LD conditions (Fig. 2C, D), revealing that the role of GNC in repressing flowering is at least partially dependent on BRM. Collectively, these data

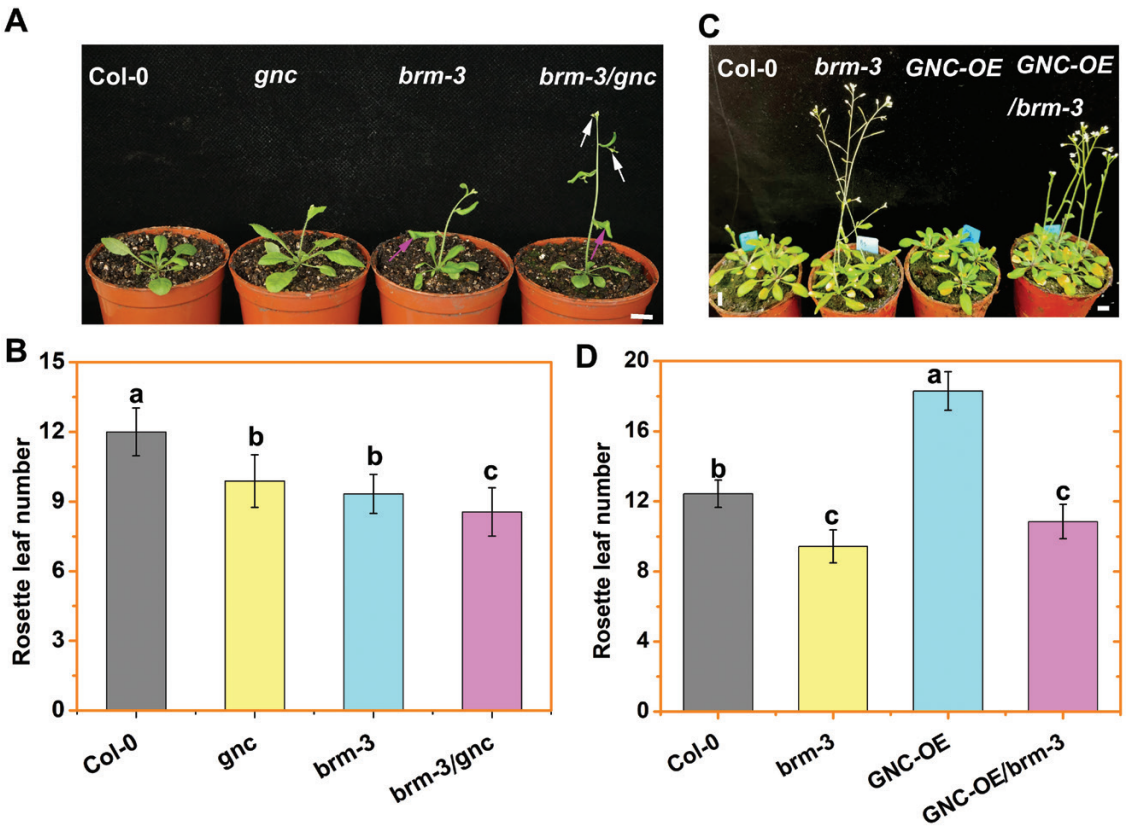

Fig. 2. Flowering time of plants grown under LD conditions. (A) Comparison of flowering phenotypes of plants with various genetic backgrounds shortly after bolting. For direct comparison, pictures of Col-0, *gnc*, *brm-3*, and *brm-3/gnc* were taken at the same time shortly after bolting of *brm-3*. All plants were grown at 22 °C under LD conditions. White arrows indicate the first bud and lateral branch of *brm-3/gnc* plants; purple arrows indicate the twisted cauline leaves of *brm-3* and *brm-3/gnc* plants. Scale bar =1 cm. (B) Rosette leaf number at bolting of plants as shown in (A). Error bar indicates SD from at least 20 plants. Lowercase letters indicate significant differences between genetic backgrounds, as determined by one-way ANOVA ($P \leq 0.05$). (C) and (D) Flowering phenotypes and rosette leaf numbers at flowering of plants with various genetic backgrounds shortly after bolting of Col-0 under LD conditions. Rosette leaf numbers were determined from at least 20 plants for each line. Values are means ±SE. Means with different letters are significantly different from each other (one-way ANOVA, $P \leq 0.05$).

demonstrate that BRM associates with GNC to regulate flowering time.

BRM and GNC are known to regulate chlorophyll biosynthesis (Richter *et al.*, 2013*a*; D. Zhang *et al.*, 2017). Therefore, we analysed the chlorophyll content of the GNC and BRM mutant and overexpression plants. Intriguingly, the chlorophyll content of the *brm-3/gnc* double mutant and *GNC*-OE/*brm-3* plants was similar to those of the *gnc* single mutant and *GNC*-OE plants, respectively (Supplementary Fig. S4). Moreover, no difference was observed between the chlorophyll content of *BRM*-OE and Col-0 (Supplementary Fig. S4). Collectively, these results suggest that GNC-mediated greening was not dependent on BRM.

BRM and GNC co-regulate SOC1 *expression*

Previous work showed that GNC regulates flowering time by repressing *SOC1* expression in Arabidopsis (Richter *et al.*, 2013*a*). We further investigated whether BRM and GNC co-regulate flowering gene expression using quantitative real-time PCR (qPCR). We analysed the expression of *SOC1* and *FT,* two potent flowering time activator genes, in 12-day-old *brm-3*, *gnc*, and *brm-3/gnc* mutants. As shown in Fig. 3A, the transcript levels of *SOC1* and *FT* were higher in the *brm-3* and *gnc* mutants than in Col-0, when using *UBQ10* as an internal control. *SOC1* expression was further increased in the *brm-3/gnc* double mutant, compared with the single mutants. Similar results were observed when using *ACTIN2* as an internal control (Supplementary Fig. S5). Interestingly, the expression of *FLC,* a repressor of floral transition and FT, was also increased in the *brm-3*, *gnc,* and *brm-3/gnc* plants, compared with Col-0 (Fig. 3A; Supplementary Fig. S5).

To test whether BRM and GNC could co-repress the transcription of a reporter gene driven by the *SOC1* promoter, we performed transient expression assays using a dual-luciferase reporter. The dual luciferase reporter plasmids contain either LUC driven by the *SOC1* promoter ($SOC1_{pro}$-LUC) or REN driven by the CaMV35S promoter as an internal control, while the pEAQ-$BRM_{1\text{-}952}$-GFP and pHB-*GNC*-FLAG plasmids were used as effectors (Fig. 3B). First, we examined

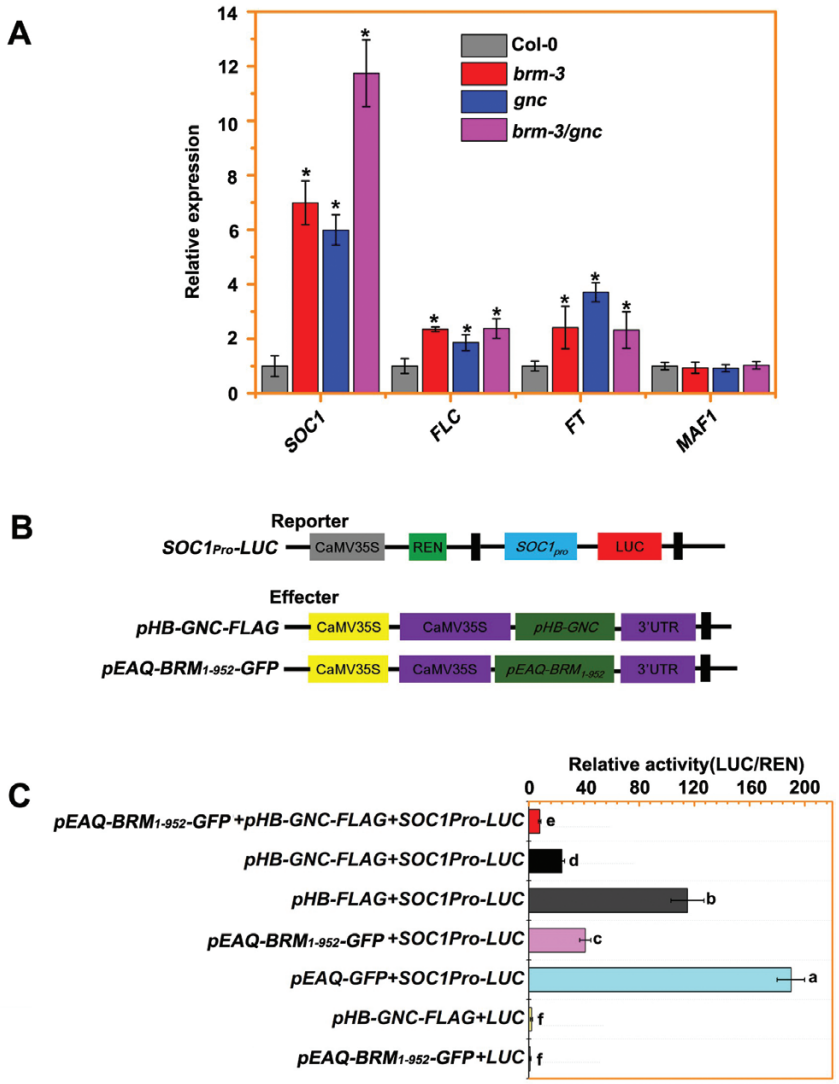

Fig. 3. BRM and GNC co-repress the expression of *SOC1*. (A) Analysis of *SOC1*, *FLC* and *FT* expression in Col-0, *brm-3, gnc*, and *brm-3/gnc* seedlings. Total RNA was extracted from 12-day-old MS cultured seedlings growing under LD conditions. *UBQ10* was used as an internal control. Data are means ±SE of three independent replicates. Asterisks indicate a significant difference between mutant and WT (Student's *t*-test, $P \leq 0.05$). (B) Diagrams of the double reporter and effector plasmid constructs used in the transient transactivation assays. (C) Transient transactivation assays of repression of *SOC1* transcription by BRM (1–952 aa) and GNC in tobacco leaves. The *Agrobacterium* (strain EHA105) carrying the indicated construct was injected into tobacco leaves. pHB-*GNC-FLAG+LUC* and pEQA-BRM_{1-952}-*GFP+LUC* represent the *Agrobacterium* carrying the effector constructs and the control vector pGreenII *0800-LUC*. The tobacco leaves were allowed to recover for 48 h, and suppression of *SOC1* promoter by BRM (1–952aa) and GNC is shown by the ratio of LUC to REN. Each value represents the mean of three biological replicates, and vertical bars represent the mean ±SE. Means with different letters are significantly different from each other (one-way ANOVA, $P \leq 0.05$).

whether BRM or GNC alone could repress *SOC1* promoter activity. The expression of BRM_{1-952}-GFP or GNC-FLAG alone resulted in decreased reporter expression from the *SOC1* promoter compared with the control of GFP or FLAG (Fig. 3C), indicating that both BRM and GNC function as transcriptional repressors of *SOC1* expression. Moreover, co-transformation with pEAQ-BRM_{1-952}-GFP and pHB-*GNC*-FLAG dramatically decreased the reporter gene expression compared with BRM or GNC alone (Fig. 3C), which is consistent with the qPCR data. Taken together, these data suggest that BRM and GNC co-repress *SOC1* expression.

BRM and GNC co-target to the promoter and coding region of SOC1

To examine whether *SOC1* is a direct target of regulation by BRM and GNC *in vivo*, we performed chromatin immunoprecipitation (ChIP) assays. Samples were taken from transgenic plants that express either green fluorescent protein (GFP)-tagged BRM driven by its native promoter (*BRMpro:BRM*-GFP; Smaczniak *et al.*, 2012; Li *et al.*, 2015) or GFP-tagged GNC driven by the CaMV35S promoter (*GNC*-GFP). An anti-GFP antibody was used for immunoprecipitation,

and we analysed the occupancy of BRM and GNC at the promoter and coding region of *SOC1* (Fig. 4A). Consistent with previous research, GNC strongly bound to the promoter region P1 and the coding region E1 of *SOC1* (Fig. 4B), indicating that *SOC1* is a direct target of GNC. Similar to GNC, we also detected a relatively high enrichment of BRM at the promoter region P1 and the coding region E1 of *SOC1* in *BRMpro:BRM*-GFP plants compared with the wild type (Fig. 4B). These results indicate that GNC and BRM co-target to *SOC1 in vivo*.

In contrast, we did not identify a significant ($P \leq 0.05$) enrichment of GNC in the coding region E2 of *SOC1* in *GNC-GFP* plants (Fig. 4B), and found no significant enrichment of BRM in the promoter region P2 or the coding region E2 of *SOC1* in *BRMpro:BRM*-GFP and *BRMpro:BRM*-GFP*/gnc* plants (Fig. 4B, C). Together, these data suggest that both BRM and GNC specifically bind to the promoter region P1 and the coding region E1 of *SOC1*.

To determine if GNC could affect the enrichment of BRM at the *SOC1* locus, or vice versa, *BRMpro:BRM*-GFP was introduced into *gnc* plants by crossing, and *GNC*-GFP into *brm-3* plants. ChIP analysis showed that in *BRMpro:BRM-GFP/gnc* plants, the association of BRM with the promoter region P1 and the coding region E1 of *SOC1* was abolished (Fig. 4C), indicating that GNC is necessary for the association of BRM to its target. In contrast, the promoter region P1 of *SOC1* was significantly ($P \leq 0.05$) enriched in *GNC*-GFP*/brm-3,* compared with *GNC*-GFP and wild-type seedlings (Supplementary Fig. S6), indicating that BRM may repress the binding of GNC to *SOC1*.

Since our data indicated that GNC is a direct transcriptional repressor that is upstream of *SOC1*, we hypothesized that the late-flowering phenotype of *soc1* may not be suppressed in the *gnc* mutant background. Indeed, no significant ($P \leq 0.05$) difference was observed between the flowering time of the *gnc/soc1* double mutant and the *soc1* mutant (Supplementary Fig. S7). Unfortunately, we were unable to create the *brm-3/soc1* double mutant, suggesting that this combination of homozygous mutations may be lethal.

BRM and GNC decrease H3K4Me3 and increase DNA methylation of SOC1

Since the H3K27Me3 demethylase REF6 can recruit BRM to its target genomic loci (Li *et al.*, 2016), we performed a ChIP assay to measure H3K27Me3 at *SOC1* in Col-0, *brm-3*, *gnc,* and *brm-3/gnc* plants. However, the level of H3K27Me3 was not significantly ($P \leq 0.05$) changed in *brm-3*, *gnc,* and *brm-3/gnc* mutants compared with Col-0 (Supplementary Fig. S8), which is consistent with a prior, genome-wide analysis of H3K27Me3 levels in 14-day-old *brm-1* mutant plants (Li *et al.*, 2015). The observation that H3K27Me3 level of *SOC1* was unchanged in *brm-3* plants indicates that the regulation of H3K27Me3 in *SOC1* may not depend on the BRM-REF6 module.

Next, we measured the level of the activation marker H3K4Me3 at *SOC1*. As shown in Fig. 5A, the H3K4Me3 levels

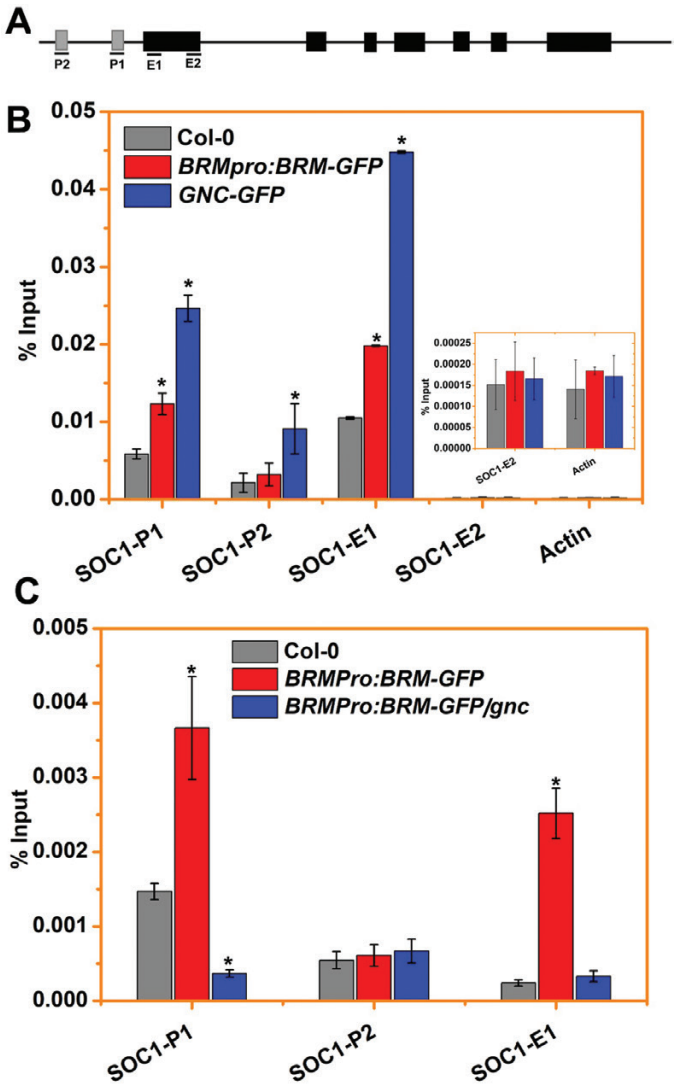

Fig. 4. BRM and GNC co-target to the promoter and coding region of *SOC1*. (A) Schematic structure of *SOC1* and the regions examined by ChIP. (B) Seedlings (12-day-old cultured on MS media) expressing *BRMpro:BRM-GFP* and *GNC-GFP* under LD conditions were used for ChIP analyses using an anti-GFP antibody. Relative enrichment was calculated based on IP/Input for each sample (% Input). The inset figure represents the zoomed in regions of *SOC1-E2* and *ACTIN2*. The x-axis represents two primers that amplified the target regions indicated in (A). *ACTIN2* was used as an internal control. (C) *BRMpro:BRM-GFP* was crossed into the *gnc* background for ChIP assays. The enrichment of DNA fragments of the promoter and coding regions of *SOC1* was examined by ChIP-qPCR assays. *ACTIN2* was used as a negative control. The values are means ±SE. Asterisks indicate significant differences (Student's *t*-test, $P \leq 0.05$).

in the promoter region P1 and the coding region E1 of *SOC1* were elevated in *brm-3, gnc,* and *brm-3/gnc* mutants compared with the wild type, especially in the *brm-3/gnc* plants. The increased H3K4Me3 levels at *SOC1* that were observed in *brm-3, gnc,* and *brm-3/gnc* plants are consistent with up-regulation of *SOC1* in these mutants. Collectively, these data suggest that BRM and GNC co-repress *SOC1* expression by decreasing the levels of H3K4Me3.

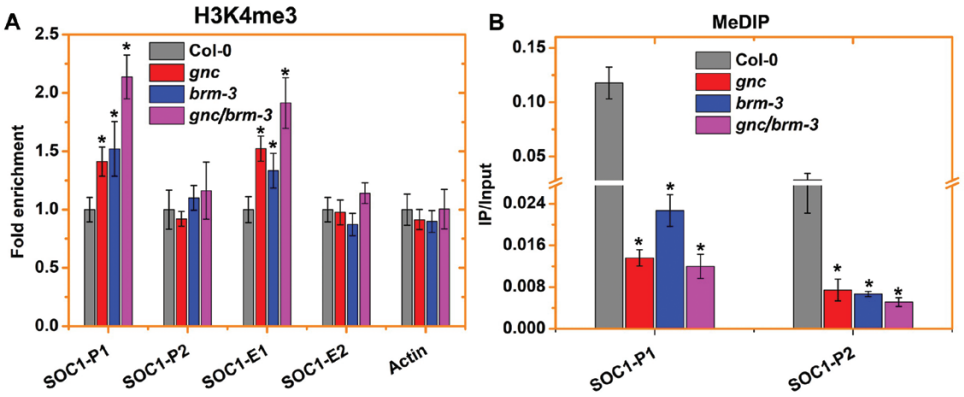

Fig. 5. BRM and GNC decrease H3K4Me3 and increase DNA methylation levels of *SOC1*. (A) ChIP-qPCR analysis of the histone H3K4Me3 level of *SOC1* locus in 12-day-old MS cultured Col-0, *brm-3, gnc*, and *brm-3/gnc* plants under LD conditions. The fold enrichment of y-axis values were calculated based on IP/Input for each sample. The *ACTIN2* was used as an internal control. (B) Methylated DNA immunoprecipitation-qPCR (MeDIP-qPCR) analysis of the DNA methylation levels of *SOC1* promotor regions in 12-day-old Col-0, *brm-3, gnc*, and *brm-3/gnc* plants. A 5-methylcytidine (5mC) antibody was used for immunoprecipitation. ChIP signals are shown as IP/Input using *ACTIN2* as an internal control. The values are means ±SE. Asterisks indicate significant differences (Student's *t*-test, $P \leq 0.05$).

Our recent work demonstrated that SWI3B, an Arabidopsis homolog of the yeast SWI3 subunit of SWI/SNF CRCs, can repress transposons by modulating the level of DNA methylation (Yang *et al.*, 2020). To examine whether BRM also affects DNA methylation, we measured DNA methylation in the P1 and P2 regions of *SOC1* by methylated DNA immunoprecipitation-qPCR (MeDIP-qPCR) using a monoclonal antibody that specifically recognizes 5-methylcytidine (Zhao *et al.*, 2014). We established that the level of DNA methylation in the *SOC1* promoter region was remarkably decreased in *brm-3, gnc,* and *brm-3/gnc* mutants, compared with Col-0 (Fig. 5B). Collectively, these data suggest that GNC and BRM repress *SOC1* by increasing DNA methylation and decreasing H3K4Me3 levels.

Discussion

In vascular plants, one of the most important developmental transitions is from the vegetative to the reproductive phase. The correct timing of flowering is crucial for the reproductive success of a plant and, therefore, a key determinant of plant fitness. Several pathways involved in regulating flowering time are affected by different endogenous cues (autonomous, gibberellin, circadian clock, age, and sugar content) and environmental stimuli (vernalization, ambient temperature, and photoperiod; Song *et al.*, 2013; Spanudakis and Jackson, 2014; Blumel *et al.*, 2015). These regulatory mechanisms converge towards a few floral integrator genes, such as *FT* and *SOC1*. As a key integrator of flowering pathways, SOC1 regulates not only flowering time but also floral patterning, floral meristem determinacy, and cold tolerance (Liu *et al.*, 2007; 2009; Seo *et al.*, 2009; Richter *et al.*, 2013*a*). In flowering, SOC1, which acts downstream of FT but upstream of LFY, is directly targeted by the floral repressor FLC and the interaction partner of FLC, SVP (Lee and Lee, 2010). Furthermore, the SVP-FLC complex directly represses *FT*, whereas *FT* interacts with the bZIP transcription factor FD to up-regulate *SOC1* directly (Abe *et al.*, 2005; Helliwell *et al.*, 2006; Tao *et al.*, 2012; Collani *et al.*, 2019).

In addition to *FLC* and *SVP*, many other factors, including epigenetic regulatory proteins, also positively or negatively directly regulate *SOC1*. For instance, the NF-Y complex binds to the *SOC1* promoter and modulates its H3K27Me3 dynamics partly via REF6 (Hou *et al.*, 2014). Moreover, SET DOMAIN GROUP 26 (SDG26), a histone methyltransferase, binds to and increases the levels of H3K4Me3 and H3K36Me3 at *SOC1*, leading to activation of this gene and thereby promoting flowering (Berr *et al.*, 2015). Here we demonstrate that the Arabidopsis chromatin remodelling ATPase BRM is also involved in flowering regulation by directly repressing the expression of *SOC1* (Fig. 3, Supplementary Fig. S5). Consistent with the early-flowering phenotype of *brm* mutants, *FT* expression is also significantly increased in *brm* mutants (Farrona *et al.*, 2011) (Fig. 3; Supplementary Fig. S5). Prior genetic data indicated that BRM can control *FT* expression independent of CO and FLC (Farrona *et al.*, 2011). Additionally, a previous study showed that BRM can activate *SVP* expression by directly binding to its promoter (Li *et al.*, 2015). Hence, a *BRM* mutation results in reduced *SVP* expression and a lower abundance of the SVP-FLC repressor complex, which ultimately leads to elevated levels of FT and SOC1, despite the increased expression of *FLC*. Our ChIP data showed that BRM specifically binds to the *SOC1* locus (Fig. 4), indicating that *SOC1* is also a direct target of BRM. Collectively, these data suggest that BRM not only represses *SOC1* directly but also indirectly, via SVP.

Previous studies indicate that BRM can be recruited to its target genes by different transcription factors (Vercruyssen *et al.*, 2014; Zhao *et al.*, 2015). Our results show that BRM can interact with the GATA family transcription factor GNC both *in vitro* and

in vivo (Fig. 1). GNC is a key regulator that is involved in chlorophyll biosynthesis, auxin and gibberellin signals, germination, greening, senescence, and flowering time in Arabidopsis (Hudson *et al.*, 2011; Richter et al., 2010; 2013*a*; Chiang *et al.*, 2012; Ranftl *et al.*, 2016). In plant greening, GNC and its homolog GNL directly activate the expression of several key enzymes in the chlorophyll biosynthesis pathway (Bastakis *et al.*, 2018), thus promoting chloroplast formation in light-grown Arabidopsis seedlings. In contrast, BRM plays a negative role in chlorophyll biosynthesis by directly repressing *PORC* in dark-grown seedlings (J. Zhang *et al.*, 2017). BRM is directly recruited to the promoter of *PORC* in the dark in a manner that is partially dependent on the transcription factor PIF1, a protein that is degraded in light. Furthermore, *BRM* expression is reduced when etiolated seedlings are transferred to the light (D. Zhang *et al.*, 2017). Collectively, these data suggest that *BRM* may not be involved in chlorophyll biosynthesis under light. Consistent with these conclusions, our data also showed that there is no difference between the chlorophyll content of *brm-3*, *BRM-OE*, and Col-0 plants under LD conditions (Supplementary Fig. S4). Moreover, the chlorophyll content did not change when *GNC* was overexpressed in *brm-3* seedlings under LD conditions. However, more research is needed to explore the function of the BRM-GNC interaction in chlorophyll biosynthesis under light.

To control flowering time, GNC directly represses *SOC1* expression by binding to the two GATA boxes in the first intron and exon of the *SOC1* promoter (Richter *et al.*, 2013*a*). Our ChIP data also show that both BRM and GNC bind to the GATA boxes of *SOC1*. Furthermore, GNC is required for the binding of BRM to *SOC1*, whereas BRM repressed the binding of GNC to *SOC1* (Fig. 4; Supplementary Fig. S6). Indeed, as the ATPase subunit of the chromatin remodelling complex, BRM cannot directly bind to DNA *in vitro* (Zhao *et al.*, 2015). Instead, the binding of BRM to DNA requires the presence of transcription factors or other DNA-binding proteins such as REF6 (Zhao *et al.*, 2015; Li *et al.*, 2016; D. Zhang *et al.*, 2017). Furthermore, other subunits of CRCs, like SWI3-like proteins (SWI3A to D), contain the SANT (SWI3, ADA2, N-CoR and TFIIIB) domain, which has a strong structural similarity to the DNA-binding domain of Myb-related proteins (Grune *et al.*, 2003). Thus, the absence of BRM may result in an 'open' chromatin state at the *SOC1* locus, which facilitates GNC binding. The *brm-3/gnc* double mutant flowers earlier than the *gnc* and *brm-3* single mutants, which is consistent with the higher expression of *SOC1* in the double mutant (Fig. 2A, B; Fig. 3).

GNC-OE plants showed a strong delayed flowering phenotype (Fig. 2C, D). In contrast, the flowering time of *GNC*-OE/*brm-3* plants was significantly earlier than that of the wild type and *GNC*-OE plants, and similar to that of the *brm-3* single mutant. These results indicate that overexpression of *GNC* has no effect on flowering when *BRM* is impaired. The dominant effect of *BRM* in flowering is consistent with the observation that BRM also acts as a direct upstream activator of SVP (Li *et al.*, 2015), which is a direct suppressor of *FT* and *SOC1*. Moreover, a previous study showed that SOC1 was involved in cold tolerance and greening by directly repressing *GNC* and *GNL* expression (Richter *et al.*, 2013*a*). Cross-repressive

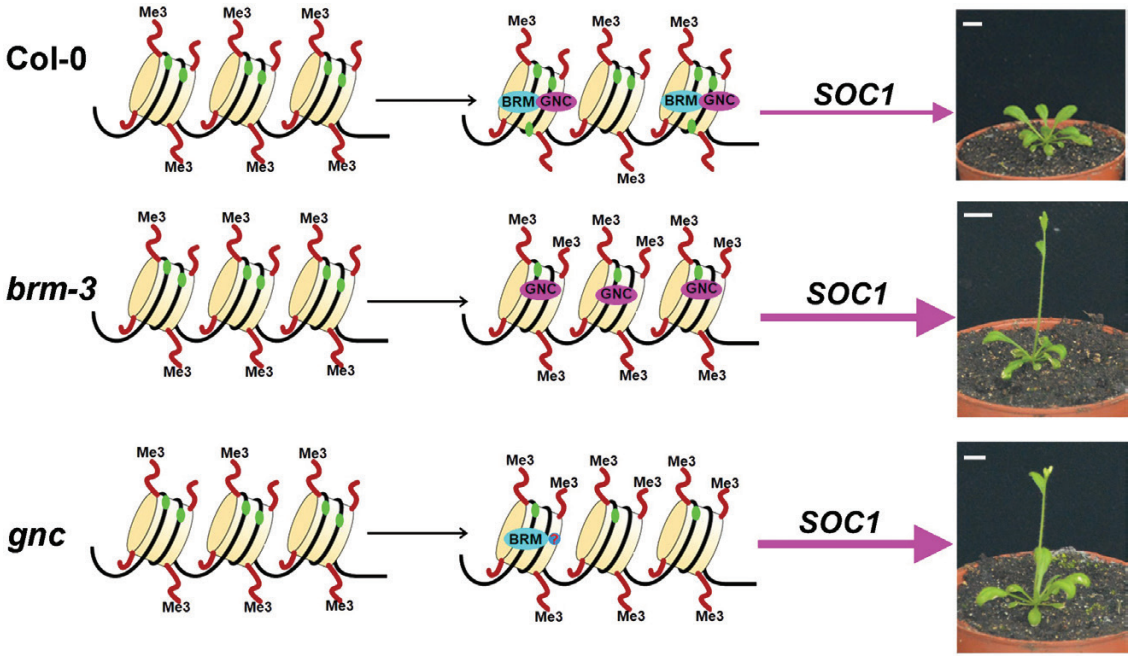

Fig. 6. A proposed model for the interaction between BRM and GNC in the regulation of *SOC1*. Scale bar =1 cm. In Col-0 plants, the chromatin remodelling ATPase BRM is recruited by the GNC transcription factor to *SOC1* to repress its expression, which is associated with decreased H3K4Me3 and increased DNA methylation at the *SOC1* locus. In *brm-3* or *gnc* mutants, since the interaction of BRM and GNC is abolished, increased H3K4Me3 and decreased DNA methylation lead to *SOC1* activation and early flowering. H3K4Me3 (Me3) and DNA methylation (green dots) are indicated. The blue cycle with the purple question mark represents unknown proteins that may interact with BRM, such as transcription factors or other subunits of the chromatin remodelling complex (e.g. SWI3C). The thickness of purple arrows indicates the expression levels of *SOC1*.

interactions, as those observed between SOC1 and GNC, were not observed between BRM and GNC, since the expression of *GNC* was not altered in *brm* mutants (Tang *et al.*, 2008; Archacki *et al.*, 2013), and the *BRM* transcript was also unchanged in *Pro35S:GNC:YFP:HA:GR* seedlings when treated with dexamethasone (Xu *et al.*, 2017). Taken together, our results suggest that BRM and GNC act additively in flowering. However, the phenotypes of *brm-3/gnc* leaves were similar to those of the *brm-3* single mutant (Fig. 2A), indicating that BRM also acts downstream of GNC in leaf development.

BRM antagonizes the functions of polycomb group (PcG) proteins through its interactions with REF6 (Li *et al.*, 2015; 2016). Thus, increased H3K27Me3 deposition at many genes is observed in *brm* mutants. However, our ChIP data showed that the level of H3K27Me3 in *SOC1* was not different between *brm-3* and the wild type (Supplementary Fig. S8), which is consistent with previous H3K27Me3 ChIP-seq data (Li *et al.*, 2015). These observations suggest that the H3K27Me3 level of *SOC1* may not depend on the BRM-REF6 module. Indeed, recent data demonstrated that SOC1, REF6, and BRM can form a complex that relaxes and opens the chromatin at *TFS1* to facilitate binding of SQUAMOSA PROMOTER BINDING PROTEIN-LIKE 9 (SPL9), and to activate poised RNA polymerase II (RNAPII), resulting in a reduction in H3K27Me3 levels across the entire *TFS1* genomic locus (Hyun *et al.*, 2016; Richter *et al.*, 2019). Interestingly, we observed that the *brm-3/gnc* mutant has a higher level of H3K4Me3 at the *SOC1* locus compared with either of the single mutants (Fig. 5), indicating that both BRM and GNC are required for the maintenance of this marker. Indeed, during the initiation of flower development, changes in H3K4Me3 prevail over changes in H3K27Me3, and quantitatively correlate with gene expression changes, while H3K27Me3 changes occur at a later stage of development (Engelhorn *et al.*, 2017). Moreover, even for PcG target genes, increases in H3K4me3 prevail during early gene activation, and H3K27Me3 remains present, while H3K4me3 is elevated (Engelhorn *et al.*, 2017).

Interestingly, the *brm-3, gnc*, and *brm-3/gnc* mutants showed lower levels of DNA methylation at the *SOC1* locus compared with the wild type (Fig. 5B), indicating that both BRM and GNC are required for the maintenance of DNA methylation. Indeed, our recent study showed that SWI3B, another subunit of the SWI/SNF chromatin-remodelling complex, interacts with the histone deacetylase HDA6, and that these proteins co-repress transposons by modulating their DNA methylation and histone modifications (Yang *et al.*, 2020). Furthermore, HDA6 was also shown to physically interact with DNA Methyltransferase 1 (MET1) and transcriptionally regulate a subset of genes, including transposons (To *et al.*, 2011; Liu *et al.*, 2012). Collectively, these observations indicate that gene regulation mediated by BRM and GNC may be involved in the cross-talk between chromatin-remodelling, DNA methylation, and histone acetylation. Nevertheless, further research is needed to explore the details of the interaction between these epigenetic marks.

In summary, we propose a working model of how the interaction between BRM and GNC contributes to flowering time control (Fig. 6). In Col-0 plants, BRM is recruited by the GNC transcription factor to *SOC1* to repress its expression, which is associated with decreased H3K4me3 and increased DNA methylation at the *SOC1* locus. In *brm-3* or *gnc* mutants, this inhibition of *SOC1* is abolished, leading to activation of *SOC1* transcription and early flowering.

Supplementary data

The following supplementary data are available at *JXB* online.

Fig. S1. The interaction between BRM and GNL was detected in yeast cells.

Fig. S2. Flowering phenotypes of Col-0, *brm-3*, and *brm-20* plants under long-day conditions.

Fig. S3. Analysis of GNC expression in Col-0, *GNC-OE*, and *GNC-OE/brm-3* plants by RT-qPCR.

Fig. S4. Chlorophyll content in Col-0, *gnc*, *brm-3*, *brm-3/gnc*, *BRM-OE*, *GNC-OE*, and *GNC-OE/brm-3* seedlings.

Fig. S5. Analysis of *FLC*, *SOC1*, *FT*, and *MAF1* expression in Col-0, *brm-3*, *gnc*, and *brm-3/gnc* mutant plants by RT-qPCR.

Fig. S6. ChIP analysis of enrichment of GNC in the different regions of *SOC1*.

Fig. S7. Flowering time of plants grown under LD photoperiod.

Fig. S8. ChIP-qPCR analysis of the histone H3K27Me3 level of SOC1 in Col-0, *gnc*, *brm-3*, and *brm-3/gnc* plants.

Table S1. Primers used in this study.

Acknowledgements

We are grateful to Dr Yawen Lei (SUN YAT-SEN UNIVERSITY) and Prof Lomonossoff (Department of Biological Chemistry, John Innes Centre, Norwich, UK) for providing the pHB and pEAQ-GFP plasmids. We thank Yuhai Cui (Southern Crop Protection and Food Research Centre, Agriculture and Agri-Food Canada) for providing *BRMpro:BRM-GFP* seeds.

Author contributions

SY, JY, YX, and KW designed the research; JY, YX, JW, SG, FH, QL, TL, and LY performed the experiments; SY, JY, KW, and YX analysed data and wrote the manuscript; SY, JY, YX, and KW revised the manuscript.

Conflict of interest

The authors declare no conflict of interest.

Funding

This work was supported by Key-Area Research and Development Program of Guangdong Province (2019B020238003, 2020B020220001);

the Open Research Fund of Guangdong Key Laboratory for New Technology Research of Vegetables (202001); Guang dong Academy of Agricultural Sciences (R2021YJ-QG001); the National Natural Science Foundation of China (No. 31672161, No.31901567); Foundation Project of President of Guangdong Academy of Agricultural Sciences (No.202021). This work was also supported by the Ministry of Science and Technology of Taiwan (108-2311-B-002-013-MY3 and 109-2311-B-002-027) and National Taiwan University (NTU-CC-110L893601).

Data availability

The data supporting the findings of this study are available from the corresponding author (SY), upon request.

References

Abe M, Kobayashi Y, Yamamoto S, Daimon Y, Yamaguchi A, Ikeda Y, Ichinoki H, Notaguchi M, Goto K, Araki T. 2005. FD, a bZIP protein mediating signals from the floral pathway integrator FT at the shoot apex. Science (New York, N.Y.) **309**, 1052–1056.

Andrés F, Kinoshita A, Kalluri N, *et al.* 2020. The sugar transporter SWEET10 acts downstream of FLOWERING LOCUS T during floral transition of *Arabidopsis thaliana*. BMC Plant Biology **20**, 53.

Archacki R, Buszewicz D, Sarnowski TJ, *et al.* 2013. BRAHMA ATPase of the SWI/SNF chromatin remodeling complex acts as a positive regulator of gibberellin-mediated responses in *Arabidopsis*. PLoS One **8**, e58588.

Bastakis E, Hedtke B, Klermund C, Grimm B, Schwechheimer C. 2018. LLM-domain B-GATA transcription factors play multifaceted roles in controlling greening in *Arabidopsis*. The Plant Cell **30**, 582–599.

Berr A, Shafiq S, Pinon V, Dong A, Shen WH. 2015. The trxG family histone methyltransferase SET DOMAIN GROUP 26 promotes flowering via a distinctive genetic pathway. The Plant Journal **81**, 316–328.

Bi YM, Zhang Y, Signorelli T, Zhao R, Zhu T, Rothstein S. 2005. Genetic analysis of *Arabidopsis* GATA transcription factor gene family reveals a nitrate-inducible member important for chlorophyll synthesis and glucose sensitivity. The Plant Journal **44**, 680–692.

Blumel M, Dally N, Jung C. 2015. Flowering time regulation in crops-what did we learn from *Arabidopsis*? Current Opinion in Plant Biology **32**, 121–129.

Chen H, Zou Y, Shang Y, Lin H, Wang Y, Cai R, Tang X, Zhou JM. 2008. Firefly luciferase complementation imaging assay for protein-protein interactions in plants. Plant Physiology **146**, 368–376.

Chiang YH, Zubo YO, Tapken W, Kim HJ, Lavanway AM, Howard L, Pilon M, Kieber JJ, Schaller GE. 2012. Functional characterization of the GATA transcription factors *GNC* and *CGA1* reveals their key role in chloroplast development, growth, and division in *Arabidopsis*. Plant Physiology **160**, 332–348.

Clapier CR, Cairns BR. 2009. The biology of chromatin remodeling complexes. Annual Review of Biochemistry **78**, 273–304.

Clapier CR, Iwasa J, Cairns BR, Peterson CL. 2017. Mechanisms of action and regulation of ATP-dependent chromatin-remodelling complexes. Nature Reviews. Molecular Cell Biology **18**, 407–422.

Clough SJ, Bent AF. 1998. Floral dip: a simplified method for Agrobacterium-mediated transformation of *Arabidopsis thaliana*. The Plant Journal **16**, 735–743.

Collani S, Neumann M, Yant L, Schmid M. 2019. FT modulates genome-wide DNA-binding of the bZIP transcription factor FD. Plant Physiology **180**, 367–380.

Efroni I, Han SK, Kim HJ, Wu MF, Steiner E, Birnbaum KD, Hong JC, Eshed Y, Wagner D. 2013. Regulation of leaf maturation by chromatin-mediated modulation of cytokinin responses. Developmental Cell **24**, 438–445.

Engelhorn J, Blanvillain R, Kröner C, Parrinello R, Rohmer M, Posé D, Ott F, Schmid M, Carles C. 2017. Dynamics of H3K4me3 chromatin marks prevails over H3K27me3 for gene regulation during flower morphogenesis in *Arabidopsis thaliana*. Epigenomes **1**, 90.

Evans T, Reitman M, Felsenfeld G. 1988. An erythrocyte-specific DNA-binding factor recognizes a regulatory sequence common to all chicken globin genes. Proceedings of the National Academy of Sciences, USA **85**, 5976–5980.

Farrona S, Hurtado L, Bowman JL, Reyes JC. 2004. The *Arabidopsis thaliana* SNF2 homolog AtBRM controls shoot development and flowering. Development **131**, 4965–4975.

Farrona S, Hurtado L, March-Díaz R, Schmitz RJ, Florencio FJ, Turck F, Amasino RM, Reyes JC. 2011. Brahma is required for proper expression of the floral repressor FLC in *Arabidopsis*. PLoS One **6**, e17997.

Farrona S, Hurtado L, Reyes JC. 2007. A nucleosome interaction module is required for normal function of *Arabidopsis thaliana* BRAHMA. Journal of Molecular Biology **373**, 240–250.

Gendrel AV, Lippman Z, Martienssen R, Colot V. 2005. Profiling histone modification patterns in plants using genomic tiling microarrays. Nature Methods **2**, 213–218.

Gietz RD, Woods RA. 2002. Transformation of yeast by lithium acetate/single-stranded carrier DNA/polyethylene glycol method. Methods in Enzymology **350**, 87–96.

Grüne T, Brzeski J, Eberharter A, Clapier CR, Corona DF, Becker PB, Müller CW. 2003. Crystal structure and functional analysis of a nucleosome recognition module of the remodeling factor ISWI. Molecular Cell **12**, 449–460.

Han SK, Sang Y, Rodrigues A,Wu MF, Rodriguez PL, Wagner D. BIOL425 F2010. 2012. The SWI2/SNF2 chromatin remodeling ATPase BRAHMA represses abscisic acid responses in the absence of the stress stimulus in *Arabidopsis*. The Plant Cell **24**, 4892–4906.

Hargreaves DC, Crabtree GR. 2011. ATP-dependent chromatin remodeling: genetics, genomics and mechanisms. Cell Research **21**, 396–420.

Hellens RP, Allan AC, Friel EN, Bolitho K, Grafton K, Templeton MD, Karunairetnam S, Gleave AP, Laing WA. 2005. Transient expression vectors for functional genomics, quantification of promoter activity and RNA silencing in plants. Plant Methods **1**, 13.

Helliwell CA, Wood CC, Robertson M, James Peacock W, Dennis ES. 2006. The *Arabidopsis* FLC protein interacts directly in vivo with SOC1 and FT chromatin and is part of a high-molecular-weight protein complex. The Plant Journal **46**, 183–192.

Hepworth SR, Valverde F, Ravenscroft D, Mouradov A, Coupland G. 2002. Antagonistic regulation of flowering-time gene *SOC1* by *CONSTANS* and *FLC* via separate promoter motifs. The EMBO Journal **21**, 4327–4337.

Ho L, Crabtree GR. 2010. Chromatin remodelling during development. Nature **463**, 474–484.

Hou X, Zhou J, Liu C, Liu L, Shen L, Yu H. 2014. Nuclear factor Y-mediated H3K27me3 demethylation of the SOC1 locus orchestrates flowering responses of *Arabidopsis*. Nature Communications **5**, 4601.

Hudson D, Guevara D, Yaish MW, Hannam C, Long N, Clarke JD, Bi YM, Rothstein SJ. 2011. GNC and CGA1 modulate chlorophyll biosynthesis and glutamate synthase (GLU1/Fd-GOGAT) expression in *Arabidopsis*. PLoS One **6**, e26765.

Hurtado L, Farrona S, Reyes JC. 2006. The putative SWI/SNF complex subunit BRAHMA activates flower homeotic genes in *Arabidopsis thaliana*. Plant Molecular Biology **62**, 291–304.

Hyun Y, Richter R, Vincent C, Martinez-Gallegos R, Porri A, Coupland G. 2016. Multi-layered regulation of SPL15 and cooperation with SOC1 integrate endogenous flowering pathways at the *Arabidopsis* Shoot Meristem. Developmental Cell **37**, 254–266.

Jerzmanowski A. 2007. SWI/SNF chromatin remodeling and linker histones in plants. Biochimica et Biophysica Acta **1769**, 330–345.

Klermund C, Ranftl QL, Diener J, Bastakis E, Richter R, Schwechheimer C. 2016. LLM-domain B-GATA transcription factors promote stomatal development downstream of light signaling pathways in *Arabidopsis thaliana* Hypocotyls. The Plant Cell **28**, 646–660.

Ko LJ, Engel JD. 1993. DNA-binding specificities of the GATA transcription factor family. Molecular and Cellular Biology **13**, 4011–4022.

Kwon CS, Hibara K, Pfluger J, Bezhani S, Metha H, Aida M, Tasaka M, Wagner D. 2006. A role for chromatin remodeling in regulation of *CUC* gene expression in the *Arabidopsis* cotyledon boundary. Development **133**, 3223–3230.

Lee J, Lee I. 2010. Regulation and function of SOC1, a flowering pathway integrator. Journal of Experimental Botany **61**, 2247–2254.

Li C, Chen C, Gao L, *et al.* 2015. The *Arabidopsis* SWI2/SNF2 chromatin remodeler BRAHMA regulates polycomb function during vegetative development and directly activates the flowering repressor gene *SVP*. PLoS Genetics **11**, e1004944.

Li C, Gu L, Gao L, *et al.* 2016. Concerted genomic targeting of H3K27 demethylase REF6 and chromatin-remodeling ATPase BRM in *Arabidopsis*. Nature Genetics **48**, 687–693.

Liu C, Xi W, Shen L, Tan C, Yu H. 2009. Regulation of floral patterning by flowering time genes. Developmental Cell **16**, 711–722.

Liu C, Zhou J, Bracha-Drori K, Yalovsky S, Ito T, Yu H. 2007. Specification of *Arabidopsis* floral meristem identity by repression of flowering time genes. Development **134**, 1901–1910.

Liu X, Yu CW, Duan J, Luo M, Wang K, Tian G, Cui Y, Wu K. 2012. HDA6 directly interacts with DNA methyltransferase MET1 and maintains transposable element silencing in *Arabidopsis*. Plant Physiology **158**, 119–129.

Lowry JA, Atchley WR. 2000. Molecular evolution of the GATA family of transcription factors: conservation within the DNA-binding domain. Journal of Molecular Evolution **50**, 103–115.

Mao J, Zhang YC, Sang Y, Li QH, Yang HQ. 2005. From The Cover: A role for *Arabidopsis* cryptochromes and COP1 in the regulation of stomatal opening. Proceedings of the National Academy of Sciences, USA **102**, 12270–12275.

Naito T, Kiba T, Koizumi N, Yamashino T, Mizuno T. 2007. Characterization of a unique GATA family gene that responds to both light and cytokinin in *Arabidopsis thaliana*. Bioscience, Biotechnology, and Biochemistry **71**, 1557–1560.

Porra R, Thompson W, Kriedemann P. 1989. Determination of accurate extinction coefficients and simultaneous equations for assaying chlorophylls a and b extracted with four different solvents: verification of the concentration of chlorophyll standards by atomic absorption spectroscopy. Biochimica et Biophysica Acta-Gene Structure and Expression **975**, 384–394.

Ranftl QL, Bastakis E, Klermund C, Schwechheimer C. 2016. LLM-domain containing B-GATA factors control different aspects of cytokinin-regulated development in *Arabidopsis thaliana*. Plant Physiology **170**, 2295–2311.

Reyes JC, Muro-Pastor MI, Florencio FJ. 2004. The GATA family of transcription factors in *Arabidopsis* and rice. Plant Physiology **134**, 1718–1732.

Richter R, Bastakis E, Schwechheimer C. 2013*a*. Cross-repressive interactions between SOC1 and the GATAs GNC and GNL/CGA1 in the control of greening, cold tolerance, and flowering time in *Arabidopsis*. Plant Physiology **162**, 1992–2004.

Richter R, Behringer C, Müller IK, Schwechheimer C. 2010. The GATA-type transcription factors GNC and GNL/CGA1 repress gibberellin signaling downstream from DELLA proteins and PHYTOCHROME-INTERACTING FACTORS. Genes & Development **24**, 2093–2104.

Richter R, Behringer C, Zourelidou M, Schwechheimer C. 2013*b*. Convergence of auxin and gibberellin signaling on the regulation of the GATA transcription factors GNC and GNL in *Arabidopsis thaliana*. Proceedings of the National Academy of Sciences, USA **110**, 13192–13197.

Richter R, Kinoshita A, Vincent C, Martinez-Gallegos R, Gao H, van Driel AD, Hyun Y, Mateos JL, Coupland G. 2019. Floral regulators FLC and SOC1 directly regulate expression of the B3-type transcription factor TARGET OF FLC AND SVP 1 at the *Arabidopsis* shoot apex via antagonistic chromatin modifications. PLoS Genetics **15**, e1008065.

Sainsbury F, Thuenemann EC, Lomonossoff GP. 2009. pEAQ: versatile expression vectors for easy and quick transient expression of heterologous proteins in plants. Plant Biotechnology Journal **7**, 682–693.

Sarnowska E, Gratkowska DM, Sacharowski SP, Cwiek P, Tohge T, Fernie AR, Siedlecki JA, Koncz C, Sarnowski TJ. 2016. The role of SWI/SNF chromatin remodeling complexes in hormone crosstalk. Trends in Plant Science **21**, 594–608.

Seo E, Lee H, Jeon J, Park H, Kim J, Noh YS, Lee I. 2009. Crosstalk between cold response and flowering in *Arabidopsis* is mediated through the flowering-time gene *SOC1* and its upstream negative regulator FLC. The Plant Cell **21**, 3185–3197.

Smaczniak C, Immink RG, Muiño JM, *et al.* 2012. Characterization of MADS-domain transcription factor complexes in *Arabidopsis* flower development. Proceedings of the National Academy of Sciences, USA **109**, 1560–1565.

Song YH, Ito S, Imaizumi T. 2013. Flowering time regulation: photoperiod- and temperature-sensing in leaves. Trends in Plant Science **18**, 575–583.

Spanudakis E, Jackson S. 2014. The role of microRNAs in the control of flowering time. Journal of Experimental Botany **65**, 365–380.

Tang X, Hou A, Babu M, *et al.* 2008. The *Arabidopsis* BRAHMA chromatin-remodeling ATPase is involved in repression of seed maturation genes in leaves. Plant Physiology **147**, 1143–1157.

Tao Z, Shen L, Liu C, Liu L, Yan Y, Yu H. 2012. Genome-wide identification of SOC1 and SVP targets during the floral transition in *Arabidopsis*. The Plant Journal **70**, 549–561.

To TK, Kim JM, Matsui A, *et al.* 2011. *Arabidopsis* HDA6 regulates locus-directed heterochromatin silencing in cooperation with MET1. PLoS Genetics **7**, e1002055.

Vercruyssen L, Verkest A, Gonzalez N, *et al.* 2014. ANGUSTIFOLIA3 binds to SWI/SNF chromatin remodeling complexes to regulate transcription during Arabidopsis leaf development. The Plant Cell **26**, 210–229.

Vignali M, Hassan AH, Neely KE, Workman JL. 2000. ATP-dependent chromatin-remodeling complexes. Molecular and Cellular Biology **20**, 1899–1910.

Wu MF, Sang Y, Bezhani S, Yamaguchi N, Han SK, Li Z, Su Y, Slewinski TL, Wagner D. 2012. SWI2/SNF2 chromatin remodeling ATPases overcome polycomb repression and control floral organ identity with the LEAFY and SEPALLATA3 transcription factors. Proceedings of the National Academy of Sciences, USA **109**, 3576–3581.

Xu Y, Guo C, Zhou B, *et al.* 2016. Regulation of vegetative phase change by SWI2/SNF2 chromatin remodeling ATPase BRAHMA. Plant Physiology **172**, 2416–2428.

Xu Z, Casaretto JA, Bi YM, Rothstein SJ. 2017. Genome-wide binding analysis of AtGNC and AtCGA1 demonstrates their cross-regulation and common and specific functions. Plant Direct **1**, e00016.

Yang J, Yuan L, Yen MR, *et al.* 2020. SWI3B and HDA6 interact and are required for transposon silencing in *Arabidopsis*. The Plant Journal **102**, 809–822.

Yang S, Li C, Zhao L, *et al.* 2015. The *Arabidopsis* SWI2/SNF2 chromatin remodeling ATPase BRAHMA targets directly to PINs and is required for root stem cell niche maintenance. The Plant Cell **27**, 1670–1680.

Zhang D, Li Y, Zhang X, Zha P, Lin R. 2017. The SWI2/SNF2 chromatin-remodeling ATPase BRAHMA regulates chlorophyll biosynthesis in *Arabidopsis*. Molecular Plant **10**, 155–167.

Zhang J, Lai J, Wang F, *et al.* 2017. A SUMO ligase AtMMS21 regulates the stability of the chromatin remodeler BRAHMA in root development. Plant Physiology **173**, 1574–1582.

Zhao M, Yang S, Chen CY, Li C, Shan W, Lu W, Cui Y, Liu X, Wu K. 2015. *Arabidopsis* BREVIPEDICELLUS interacts with the SWI2/SNF2 chromatin remodeling ATPase BRAHMA to regulate KNAT2 and KNAT6 expression in control of inflorescence architecture. PLoS Genetics **11**, e1005125.

Zhao MT, Whyte JJ, Hopkins GM, Kirk MD, Prather RS. 2014. Methylated DNA immunoprecipitation and high-throughput sequencing (MeDIP-seq) using low amounts of genomic DNA. Cellular Reprogramming **16**, 175–184.

Zhu Y, Rowley MJ, Böhmdorfer G, Wierzbicki AT. 2013. A SWI/SNF chromatin-remodeling complex acts in noncoding RNA-mediated transcriptional silencing. Molecular Cell **49**, 298–309.

Zubo YO, Blakley IC, Franco-Zorrilla JM, Yamburenko MV, Solano R, Kieber JJ, Loraine AE, Schaller GE. 2018. Coordination of chloroplast development through the action of the GNC and GLK transcription factor families. Plant Physiology **178**, 130–147.